Research Article

Cancer Immunology Research

Extensive Profiling of the Expression of the Indoleamine 2,3-Dioxygenase 1 Protein in Normal and Tumoral Human Tissues

Ivan Théate[1,2], Nicolas van Baren[1,2], Luc Pilotte[1,2], Pierre Moulin[3], Pierre Larrieu[1,2], Jean-Christophe Renauld[1,2], Caroline Hervé[1,2], Ilse Gutierrez-Roelens[4], Etienne Marbaix[2,3,4], Christine Sempoux[3], and Benoît J. Van den Eynde[1,2]

Abstract

Tryptophan catabolism by indoleamine 2,3-dioxygenase 1 (IDO1) plays a key role in tumoral resistance to immune rejection. In humans, constitutive expression of IDO1 has been observed in several tumor types. However, a comprehensive analysis of its expression in normal and tumor tissues is still required to anticipate the risks and potential benefits of IDO1 inhibitors. Using a newly validated monoclonal antibody to human IDO1, we performed an extensive immunohistochemical analysis of IDO1 expression in normal and tumor tissues. In normal tissues, IDO1 was expressed by endothelial cells in the placenta and lung and by epithelial cells in the female genital tract. In lymphoid tissues, IDO1 was expressed in mature dendritic cells with a phenotype ($CD83^+$, DC-$LAMP^+$, $langerin^-$, $CD123^-$, $CD163^-$) distinct from plasmacytoid dendritic cells. Importantly, IDO1-expressing dendritic cells were not enriched in tumor-draining lymph nodes, in contrast with previously reported findings. IDO1-expressing cells were observed in a large fraction (505/866, 58%) of human tumors. They comprised tumor cells, endothelial cells, and stromal cells in proportions that varied depending on the tumor type. Tumors showing the highest proportions of IDO1-immunolabeled samples were carcinomas of the endometrium and cervix, followed by kidney, lung, and colon. This hierarchy of IDO1 expression was confirmed by gene expression data mined from The Cancer Genome Atlas database. Expression of IDO1 may be used to select tumors likely to benefit from targeted therapy with IDO1 inhibitors. *Cancer Immunol Res; 3(2); 161–72. ©2014 AACR.*

Introduction

Tryptophan-2,3 dioxygenase (TDO2) and indoleamine 2,3-dioxygenase 1 (IDO1) are the two main enzymes that catalyze the first and rate-limiting step in the kynurenine pathway, leading to the degradation of the essential amino acid tryptophan (1). TDO2 is expressed constitutively in the liver, where it acts as the main regulator of systemic tryptophan levels. The nonhomologous IDO1 enzyme is expressed in the placenta, the mucosal and lymphoid tissues, and inflammatory lesions (2, 3). In the latter two, it is expressed primarily by antigen-presenting cells (APC), mainly dendritic cells (DC) and macrophages, and in cells exposed to IFNγ and other proinflammatory stimuli. Local IDO1-mediated degradation of tryptophan is thought to reduce the bioavailability of tryptophan for pathogens, thus contributing to protection against infection (4). It also appears to have a profound influence on local innate and adaptive immune responses (5). T cells exposed to tryptophan depletion activate GCN2 kinase, a sensor of amino acid shortage that induces a stress response, resulting in impaired T-cell proliferation and effector functions. In addition, tryptophan catabolites such as kynurenine downregulate T-cell responses by interfering with DC function and by promoting regulatory T cell (Treg) differentiation and apoptosis of $CD4^+$ T-helper 1 (Th1) cells (5, 6). These observations indicate that IDO1 orchestrates an immunosuppressive local environment, presumably aimed at preventing exaggerated T-cell responses. IDO1 knockout mice, however, do not show signs of overt autoimmunity, indicating that IDO1 biology remains incompletely understood (7, 8).

The immunosuppressive effect of IDO1 was demonstrated first in a mouse model of fetal protection against maternal immune rejection. Treatment of pregnant mice with a tryptophan analogue that inhibits IDO1, which is constitutively expressed in the placenta, resulted in T-cell–mediated rejection of allogeneic embryos (9). We extended this concept to malignant diseases by showing that mouse tumor cells expressing IDO1 resisted immune rejection by immunized mice. In addition, we demonstrated that this inhibition could be partially reversed by

[1]Ludwig Institute for Cancer Research, Brussels Branch, Brussels, Belgium. [2]de Duve Institute, Université catholique de Louvain, Brussels, Belgium. [3]Service d'anatomopathologie, Cliniques Universitaires Saint-Luc, Brussels, Belgium. [4]Biolibrary, Université catholique de Louvain, Brussels, Belgium.

Note: Supplementary data for this article are available at Cancer Immunology Research Online (http://cancerimmunolres.aacrjournals.org/).

I. Théate and N. van Baren contributed equally to this article.

Current address for I. Théate: Institut de Pathologie et Génétique, Gosselies, Belgium; current address for C. Hervé: GlaxoSmithKline Vaccines, Rixensart, Belgium; and current address for P. Moulin: Novartis Institute of Biomedical Research, Basel, Switzerland.

Corresponding Author: Benoît J. Van den Eynde, Ludwig Institute for Cancer Research, Av. Hippocrate, 75 Bte B1.74.03, B-1200 Brussels, Belgium. Phone: 32-2-764-7572; Fax: 32-2-764-7590; E-mail: benoit.vandeneynde@bru.licr.org

doi: 10.1158/2326-6066.CIR-14-0137

pharmacologic inhibition of IDO1. We showed that IDO1 was constitutively expressed and enzymatically active in several human tumor cell lines. We raised a rabbit polyclonal antibody against IDO1 for IHC, and showed immunoreactivity in various human tumors (10).

Several mechanisms have been proposed to explain how IDO1 may favor tumor growth and survival. The immunosuppressive properties described above may protect the tumor against T-cell–mediated destruction, either through the expression of IDO1 in the tumor environment or in tumor-draining lymph nodes (TDLN). Recently, a role for IDO1 in tumor resistance against immune checkpoint blockade has been demonstrated in a murine model (11). In this model, CTLA-4 and IDO1 inhibition synergized to induce T-cell–mediated rejection of both $IDO1^+$ and $IDO1^-$ tumor cells, highlighting the immunosuppressive effect of IDO1 expression by noncancerous cells of the tumor stroma. IDO1 could also act in favor of tumors through a nonimmunologic mechanism, as tryptophan-derived kynurenine was shown to promote tumor cell survival and motility through activation of the aryl hydrocarbon receptor (6). Independent from its catalytic potential, IDO1 was shown in murine experiments to act as a signaling molecule in TGFβ-mediated immune suppression (12). Taken together, these observations provide a strong rationale for the clinical development in oncology of drugs that inhibit IDO1 and more particularly its catalytic activity, alone or in combination with other immunotherapy approaches such as CTLA4-blocking agents (13). Such IDO1 inhibitors are currently in the early phases of clinical testing.

To identify the best candidate tumors for IDO1-inhibitory therapy and evaluate its risks, it is important to have a comprehensive picture of the pattern of IDO1 expression and of the nature of IDO1-expressing cells in normal and tumoral human tissues. A lot of attention has been devoted to the study of IDO1 expression and function in DCs (reviewed in ref. 14). In inflamed and lymphoid tissues, DCs are the main contributors of IDO1 expression. Mature myeloid DCs are the most frequently cited (15–17), but IDO1 expression has also been reported in plasmacytoid DCs, immature DCs, and macrophages (18–20). Several studies have shown that $IDO1^+$ cells were enriched in melanoma-draining lymph nodes (18, 21–23). Some studies also reported a correlation between high IDO1 expression in TDLN and poor clinical outcome of melanoma, suggesting that IDO1 contributes to immune evasion (22–24). However, another study performed in breast cancer did not show an enrichment of $IDO1^+$ cells in TDLN (25). IDO1 expression and enzymatic activity in the placenta are well established, but there is still controversy about the nature of the cells that express it. IDO1 immunoreactivity has been reported in trophoblast cells, macrophages, and mesenchymal or endothelial cells, depending on the study (3, 26–31). In human tumors, most published studies have focused on IDO1 expression and prognostic significance in individual tumor types. In general, IDO1 expression was associated with a less favorable prognosis, with more aggressive features of the tumor, and with reduced immune cell infiltration or increased numbers of Tregs (reviewed in ref. 32). Of note, many of these studies relied on a limited number of patient samples, the method used to assess IDO1 expression was different from one study to the other, and the proportions of positive tumors as well as the nature of the IDO1-expressing cells were not always consistent (Supplementary Table S1).

In summary, our current knowledge of IDO1 expression in normal and tumoral human tissues is incomplete, and several inconsistencies appear when the results of different studies are compared. It is likely that experimental differences and the diversity and lack of specificity of anti-IDO1 antibodies used in IHC studies account for these differences. We provide here an extensive analysis of IDO1 protein expression in human normal tissues, including lymphoid organs. To this end, we have produced a new murine mAb that stains IDO1 in human tissue sections and have validated its specificity. We have compared and quantified IDO1-expressing DCs in normal and TDLNs. We have also analyzed the expression and activity of IDO1 in human monocyte-derived DCs *in vitro*. Lastly, we have screened the expression of IDO1 in a large panel of common human tumors.

Materials and Methods

Patients and tissue samples

Normal tissue samples were obtained from routine biopsy, surgical resection, autopsy, or obstetric materials. All cases were verified histologically to ensure that no lesion was present. The clinical characteristics of the patients from whom TDLNs were obtained are summarized in Supplementary Table S2. Tissue microarrays (TMA) were constructed from formalin-fixed paraffin-embedded (FFPE)–archived tumor pathology specimens. Briefly, tissue carrots of 3- or 5-mm in diameter were cut in tumor areas previously identified on hematoxylin–eosin-stained sections, using a manual arrayer (Quick-Ray; Unitma). Each TMA section contained between 15 and 30 single individual tissue cores. Ethical approval for the use of human biologic material was obtained from the Institutional Review Board (Commission d'Ethique Biomédicale Hospitalo-Facultaire of Université catholique de Louvain).

Plasmid constructs and cell transfectants

The complete IDO1 coding sequence was amplified from human placenta RNA by RT-PCR using sense primer 5′-GAGGAGCAGACTACAAGAATG-3′ and antisense primer 5′-GCATACAGATGTCTCTGCTATG-3′. The PCR product was cloned into pEF6/V5-His TOPO (Invitrogen) and verified by DNA sequencing. 293-EBNA cells (Invitrogen) were transfected by electroporation with the IDO1-expressing plasmid, and transfectants were selected with 5 μg/mL of blasticidin and 400 μmol/L 1-methyl-DL-tryptophan (Sigma-Aldrich). Clones obtained by limiting dilution were amplified in the presence of 1-methyl-DL-tryptophan.

To prepare an immunogen for antibody generation, the DNA sequence encoding the first 161 amino acids of human IDO1 was amplified by PCR from the full-length IDO1 cDNA with primers 5′-CAGACTTCTAGAATGGCACACGCTATG-3′ and 5′-GACCAGGGCGGCCGCTTTACTGCAGTCTCCATC-3′. The PCR product was inserted into the pCD1 expression vector, downstream of the human CD134L coding sequence (33, 34). The plasmid construct, which encodes the CD134L–$hIDO1_{1\text{-}161}$ fusion protein, was verified by sequencing.

Western blotting

Cell pellets were lysed in lysis buffer (Cytobuster; Novagen) and centrifuged for 5 minutes at 16,000 *g* at 4°C. The protein concentration of the clear supernatant was estimated using the bicinchoninic acid protein assay (Pierce). Proteins (20 μg) from

each sample were separated on NuPAGE 10% bis-tris gels (Invitrogen) and transferred onto a nitrocellulose membrane (Hybond ECL; Amersham). The membrane was blocked with PBS + 5% dry milk + 0.1% Tween 20 and probed overnight with one of three anti-IDO1 antibodies: a new batch of rabbit polyclonal antibody raised in-house as in ref. 10 (batch 718, diluted 1:500), our mouse 4.16H1 mAb (10 μg/mL), or a commercial rabbit polyclonal antibody (AB5968; Chemicon; 1:20,000). After three washings in PBS 0.1% + Tween 20, the membrane was probed for one hour with horseradish peroxidase (HRP)–linked anti-mouse (Santa Cruz Laboratories; 1:2,000) or anti-rabbit (Cell Signaling Technology; 1:5,000) antibody and revealed with SuperSignal West Pico-10% West Femto Chemiluminescent Substrate (Pierce). Actin controls were obtained after 20-minute stripping of the same nitrocellulose membranes (Restore Western blot buffer; Pierce), overnight hybridization with an anti–β-actin mAb (clone AC-15; Sigma-Aldrich; 1:10,000), and the same revelation as above.

Immunohistochemistry

After deparaffinization and rehydration of 5-μm sections from normal tissues, antigen retrieval was performed by heating at 95°C in 0.01 mol/L citrate buffer pH 5.8 and 0.05% Triton X-100 in a water bath for 75 minutes. After washing in TBS (0.05 mol/L, pH 7.4), endogenous peroxidase was blocked in 0.3% H_2O_2 (30 minutes), and nonspecific staining was prevented by preincubation in 10% normal goat serum (NGS)-TBS (30 minutes). Sections were first incubated with the 4.16H1 mAb (50 μg/mL) or, for double staining, with the in-house anti-IDO1 rabbit polyclonal antibody (batch 718, 1:300 in 1% NGS-TBS) overnight at 4°C. The second incubation was done using anti-rabbit or anti-mouse immunoglobulins conjugated to peroxidase on a dextran polymer (EnVision; Dako). Finally, peroxidase activity was revealed by TBS containing 0.05% diaminobenzidine (DAB; Fluka) and 0.01% H_2O_2. After counterstaining with hematoxylin and mounting, the images were captured with a digital Axiocam camera mounted on an Axioplan Photomicroscope and processed by the Axiovision software (all from Zeiss).

Tumor TMA sections were cut from TMA blocks (see above), mounted onto glass slides, deparaffinized, and rehydrated. Antigen retrieval was performed by heating for 1 hour at 97°C in Target Retrieval Solution, pH 9 (Dako). Endogenous peroxidase activity was blocked with Peroxidase Blocking Reagent (Dako). TMA sections were incubated for 1 hour at room temperature with unlabeled 4.16H1 anti-IDO1 antibody (2 μg/mL), washed, and incubated for 30 minutes with a secondary polyclonal goat anti-mouse antibody coupled to HRP (Envision; Dako). After washing, bound antibodies were detected with 3-amino-9-ethylcarbazole (AEC), and sections were counterstained with hematoxylin. Normal placenta was used as a positive control. Negative controls included omission of primary antibody on duplicate placenta and TMA sections. Stained slides were mounted and digitized with a SCN400 slide scanner equipped with a 20× objective (Leica). Image analysis was carried out with the SlidePath Gateway software (Leica). Tumor areas were identified on an adjacent section colored by hematoxylin and eosin. Assessment of $IDO1^+$ cells was done manually, by comparison with the negative control. TMA sections were considered positive if they contained at least one of the following features: (i) ≥1% of stained tumor cells, (ii) >5 stained tumor blood vessels, (iii) >5 tumor stromal areas containing stained cells. The same conditions were applied to the normal lung sample (Supplementary Fig. S2).

Computerized sequential immunohistochemistry for double stainings

Tissues were processed using the same preincubation steps as for normal tissues except that endogenous biotins were blocked with avidin-biotin kit (Vector Laboratories). The sections were first incubated overnight with mouse anti-CD1a mAbs (clone 010; Dako; 1:4), CD83 (clone 1H4b; Novocastra; 1:20), CD123 (clone 6H6; eBioscience; 1:10), CD163 (clone 10D6; Novocastra; 1:200), or langerin (clone 12D6; Novocastra; 1:20) antibodies or rat anti–DC-LAMP mAbs (clone 1010E1-01; Abcys; 1:50). MAbs against CD31 (clone JC70A; Dako; 1:150), cytokeratins (clone AE1/AE3; Dako; 1:100), CD68 (clone PGM1; Dako; 1:200), and α-actin (clone 1A4; Dako; 1:200) were also used to characterize positive cells in the placenta, thymus, and liver. After TBS washing, the revelation was carried out in two steps. First, sections were treated with biotin-conjugated goat anti-mouse IgG (Vector, 1:500) or biotin-conjugated sheep anti-rat F(ab′2) (Boehringer; 1:200), washed, and incubated with streptavidin–alkaline phosphatase conjugate (Dako; 1:100), both for 30 minutes. The alkaline phosphatase activity was revealed with FastRed, levamisole, and naphtol phosphate in Tris buffer 0.05 mol/L (Sigma-Aldrich). Slides were mounted immediately (Fluorescent mounting medium; Dako). High-magnification (40×/0.65 objective) images of representative fields were taken using a Zeiss microscope equipped with a scanning stage and a 3CCD video camera (KY-F58; JVC). A script was developed for this study in the KS-400 image analysis system (Zeiss vision) to record the exact position on the scanning stage for each image. Second, after image capture, FastRed (red color) was removed by immersing slides into ethanol, followed by blockade of nonspecific binding and incubation with our anti-IDO1 polyclonal rabbit antibody, as described above. IDO-1 was revealed in brown using EnVision and DAB, and images were captured at spatial coordinates recorded previously, thereby producing a set of strictly superimposable pictures. The inverse of the FastRed and DAB monochrome images was used as red and green channels of a new pseudocolor picture.

Quantitative analysis of IDO1 staining in TDLNs

Staining for IDO1 was quantified with the ImageJ software (http://rsb.info.nih.gov//ij/) on slides without counterstaining. Five digitalized pictures were obtained for each case in fields containing the highest proportions of stained cells (hot spots). The relative stained area was determined by calculating the ratio of surface staining for IDO1 to the overall surface.

***In vitro* generation of monocyte-derived DCs**

Peripheral blood mononuclear cells (PBMC) were isolated from buffy-coat collections obtained from hemochromatosis patients, and purified by density gradient centrifugation on Lymphoprep (Axis-Shield). Monocytes were isolated using anti–CD14-coated microbeads (Miltenyi Biotec), and were differentiated *in vitro* to immature DCs (iDC) during 5 days in RPMI medium supplemented with 10% FCS, L-arginine (116 mg/L), L-asparagine (36 mg/L), L-glutamine (216 mg/L), 70 ng/mL granulocyte-macrophage colony-stimulating factor, and 20 U/mL IL4. iDCs were matured during 2 days with IFNγ (500 U/mL), lipopolysaccharide (LPS; 100 ng/mL), prostaglandin-E2 (PGE2; 1 μg/mL), IL1β (10 ng/mL), IL6 (25 ng/mL), and TNFα (10 ng/mL).

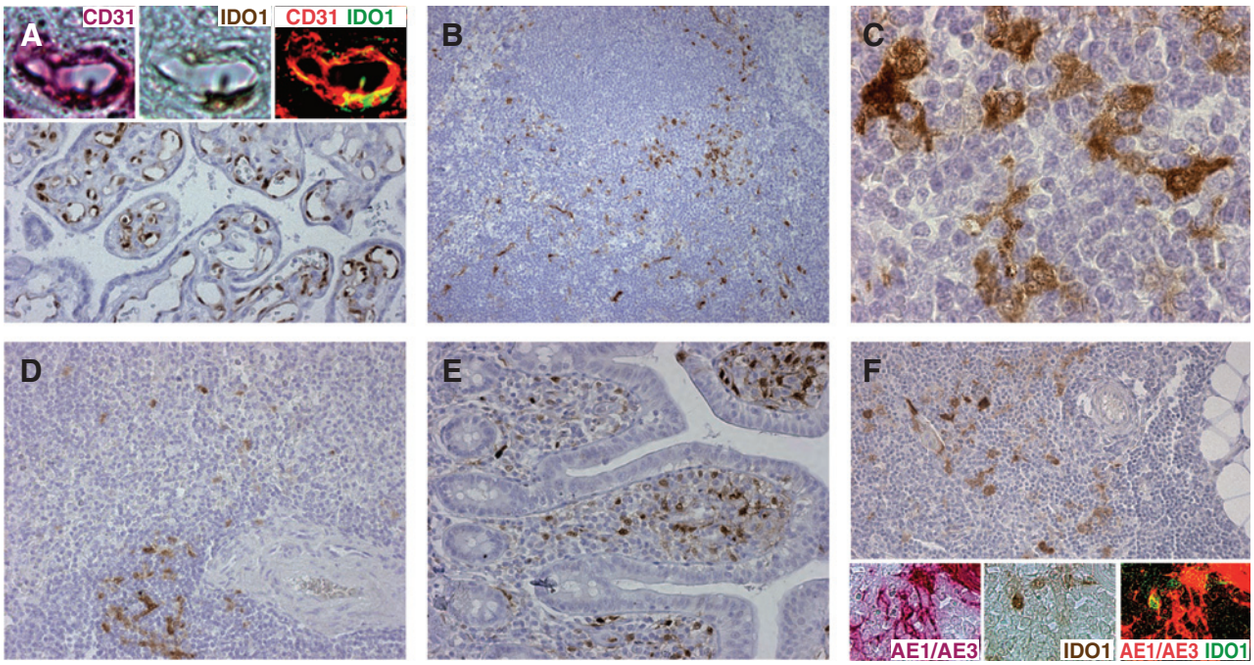

Figure 1.
IDO1 staining in normal tissues. FFPE sections of placenta (A), lymph nodes (B and C), spleen (D), small intestine (E), and thymus (F) were stained with the 4.16H1 antibody. Positive signals appear in brown (DAB staining). CD31 and IDO1 staining of placenta was colocalized by CslHC, where CD31, IDO1, and their colocalization appear in red, green, and yellow, respectively (A, insets). The same analysis was performed in thymus with cytokeratin AE1/AE3 as marker of thymic epithelial cells (F, insets). Original magnification, ×400; objectives ×20/0.5 (A–C and F), ×10/0.3 (D), and ×40/0.75 (E).

Flow cytometry

DCs were stained with fluorescent-conjugated antibodies specific for CD11c (clone S-HCL-3; BD Pharmingen), CD14 (clone M5E2; BD Pharmingen), CD40 (clone 5C3; BD Pharmingen), CD80 (clone L307.4; BD Pharmingen), CD83 (clone HB15a; Beckman Coulter), and CD86 (clone HA5.2B7; Beckman Coulter). Negative controls used isotype-matched IgG1 (clone MOPC-21; BD Pharmingen), IgG2a (clone G155-178; BD Pharmingen), and IgG2b (clone 27–35; BD Pharmingen). After staining, cells were washed and resuspended in paraformaldehyde and analyzed on FACSCalibur (BD Biosciences).

Cytokine measurement

Monocytes were cultured in growth medium as described. At day 6, 100 ng/mL LPS (Sigma-Aldrich) was added to the iDCs. Cytokine release was measured in the supernatant with a Cytometric Beads array kit on a Bio-Plex instrument (Bio-Rad Laboratories).

IDO1 activity

A total of 4×10^5 cells were seeded in 96-well plate in 200 µL Hank's Balanced Salt Solution (HBSS) + 80 µmol/L tryptophan per well. Tryptophan and kynurenine concentrations were measured by high-performance liquid chromatography (HPLC) in the supernatant immediately and after 24 hours.

Quantitative RT-PCR analysis of mRNA expression

IDO1 and *TDO2* gene expression was quantified by RT-qPCR as described (10, 35). Indoleamine 2,3-dioxygenase 2 (IDO2) transcripts were measured similarly using the following forward primer, reverse primer, and primers and probe, respectively: 5′-GTGCTGACGAACTGGACCAAAAAAG-3′, 5′-CATTGCTGGGTTGTCTTTCCATCC-3′, FAM-5′-TGGAAATTGGGAACCTGGAGACCATCATCTCATTTCCTGG-3′-TAMRA.

T-cell proliferation assays

For the $CD4^+$ T-cell proliferation assay (Supplementary Fig. S3), monocyte-derived DCs were prepared as described above. Supernatants were collected after 48 hours. $CD4^+$ lymphocytes were sorted using anti-CD4 microbeads (Miltenyi Biotec). The $CD4^+$ cells (2×10^5 cells/well) were resuspended in 100 µL of tryptophan-depleted DMEM medium (Gibco) and mixed with 100 µL of conditioned DC medium. They were activated in 96-well plates coated with anti-CD3 antibody (10 µg/mL). After 3 days, proliferation was assessed by $[H^3]$-thymidine (10 µCi/w in HBSS) uptake overnight. Each condition was tested in triplicate. For the inhibitory assay (Supplementary Fig. S4), DCs matured with 100 ng/mL LPS and 250 U/mL IFNγ were used to stimulate PBMCs in the presence of the indicated tryptophan analogues. Each condition was tested in duplicate. Proliferation was measured after 5 days by $[H^3]$-thymidine uptake.

The Cancer Genome Atlas data mining

Normalized total mRNA counts for main tumor types were derived from whole transcriptome datasets generated by The Cancer Genome Atlas (TCGA) Research Network (http://cancergenome.nih.gov), downloaded from the Cancer Browser website (https://genome-cancer.ucsc.edu/proj/site/hgHeatmap/).

The IDO1 mRNA counts transformed to linear values were represented in horizontal boxplot graphs using Microsoft Excel.

Results

Production and validation of a murine mAb directed against human IDO1

BALB/c mice were immunized with P815 mouse mastocytoma cells transfected with a CD134L–hIDO1$_{1\text{-}161}$ plasmid construct. This construct induces the expression of a chimeric protein comprising amino acids 1 to 161 of the human IDO1 protein, fused to the transmembrane segment of CD134L, in such a way that the folded IDO1 polypeptide is exposed at the external surface of the transfected cells. As opposed to immunization protocols based on synthetic peptides, this approach allows the generation of antibodies that recognize conformational epitopes within the target protein (33, 34). The selected hybridoma clone 4.16H1 derived from immunized mice produced an IgG1k antibody that on Western blot stained a unique band of the expected 40- to 45-kDa size in 293 cells transfected with the human IDO1 cDNA, but not in untransfected 293 cells (Supplementary Fig. S1A). Similar results were obtained with an in-house rabbit polyclonal anti-IDO1 antibody. However, a rabbit antiserum (AB5968 from Chemicon International), previously used to assess IDO1 expression in DCs and in placenta (18, 21), stained an additional band both in IDO1-positive and IDO1-negative cells, indicating a lack of specificity. Consistent results were obtained with IHC (Supplementary Fig. S1A). We conclude that the 4.16H1 mAb recognizes the human IDO1 protein specifically.

IDO1 expression in normal tissues

Although the expression and enzymatic activity of IDO1 in human placenta are well established, there is controversy about its cellular localization. When we stained placental tissue sections with the 4.16H1 antibody, only endothelial cells and some mesenchymal cells were positive (Fig. 1A). We found no expression in the trophoblast of term placenta. We confirmed endothelial expression with computerized sequential IHC (CsIHC) using CD31 and IDO1 staining on the same tissue section (Fig. 1A, inset). In this case, the IDO1 staining was performed with our rabbit polyclonal antibody to avoid cross-staining with the mouse anti-CD31 antibody. CsIHC was preferred to immunofluorescence as the latter is not optimal for FFPE sections. We next tested a large series of normal human tissues by IHC using our validated 4.16H1 mAb (Table 1). Consistent with previous reports (29), IDO1 was detected in some scattered cells in the glandular epithelium of the female reproductive tract, and in lymphoid organs, including lymph nodes, spleen, tonsils, Peyer's patches, the gut lamina propria, and the thymus (Fig. 1B–F). In lymph nodes, tonsils, and Peyer's patches, IDO1 staining was mainly observed in paracortical T-cell areas (Fig. 1B) in cells that were larger than lymphocytes and tended to have an irregular outline compared with lymphocytes (often stellate cells with ramified cytoplasmic expansions; Fig. 1C). The spleen contained numerous IDO1-expressing cells in periarteriolar lymphocyte sheaths and some scattered positive cells in the Billroth's cords (Fig. 1D). The lamina propria of the duodenum, small, and large intestine contained interstitial mononuclear IDO1-positive cells, which were larger than lymphocytes (Fig. 1E). CsIHC for IDO1 and DC-LAMP showed that most (>50%) of these cells were mature DCs (data not shown). In the thymus, the expression of IDO1 was restricted to the medulla (Fig. 1F). Numerous interstitial cells, morphologically different from lymphocytes, were strongly positive, whereas a weak positivity was observed in rare epithelial cells, including Hassal's bodies, as confirmed by CsIHC for IDO1 and cytokeratin (Fig. 1F, inset). In the bone marrow, we only observed a weak IDO1 expression in very few cells, which could correspond to some stromal or DCs (data not shown). In non-lymphoid organs, IDO1$^+$ cells were consistently observed within interstitial lymphocyte aggregates (data not shown). IDO was also detected in endothelial cells of many blood vessels in the lung alveolar tissue (Supplementary Fig. S2) and of a few blood vessels in the prostate and uterus (data not shown). IDO1 was recently reported to be expressed at high levels in mouse epididymis (36). We observed no staining in human epididymis (Table 1), and we confirmed the lack of expression of the *IDO1* gene by RT-qPCR in two human epididymis samples (data not shown).

Table 1. IDO1 expression assessed by IHC in normal tissues (10 samples each)

Organ, tissue	IDO-expressing cells
Placenta	Endothelial cells
Digestive tract	
Salivary glands	None
Esophagus	None
Stomach	None
Duodenum	Interstitial cells in lamina propria
Small bowel	Interstitial cells in lamina propria (DCs)
Colon	Interstitial cells in lamina propria
Pancreas	Rare endothelial cells, rare acinar cells
Gallbladder	None
Liver	<1% Intrasinusoidal cells (Kupffer cells)
Respiratory tract	
Larynx	None
Pharynx	None
Trachea	None
Bronchus	None
Lung	Endothelial cells
Urogenital system	
Kidney	None
Bladder	None
Prostate	Rare endothelial cells
Epididymis	None
Testis	None
Cervix	Rare glandular cells
Uterus	Glandular cells (30%), rare endothelial cells
Fallopian tube	Epithelial cells (10%)
Hematopoietic and lymphoid systems	
Bone marrow	Rare stromal cells (<1%)
Lymph node	Interstitial cells in paracortical areas (DCs)
Spleen	Interstitial cells in periarteriolar T-cell zone in white pulp and scattered cells in Billroth cord
Thymus	Interstitial cells in the medulla, rare epithelial cells (<1%)
Tonsils	Interstitial cells in paracortical areas
Peyer's patch	Interstitial cells in paracortical areas
Other	
Skin	None
Breast	None
Brain	None
Eye	None

Characterization of IDO1-positive cells in normal lymph nodes

In lymph nodes, the morphology of IDO1$^+$ cells in the paracortical T-cell zone was reminiscent of interdigitating DCs. By

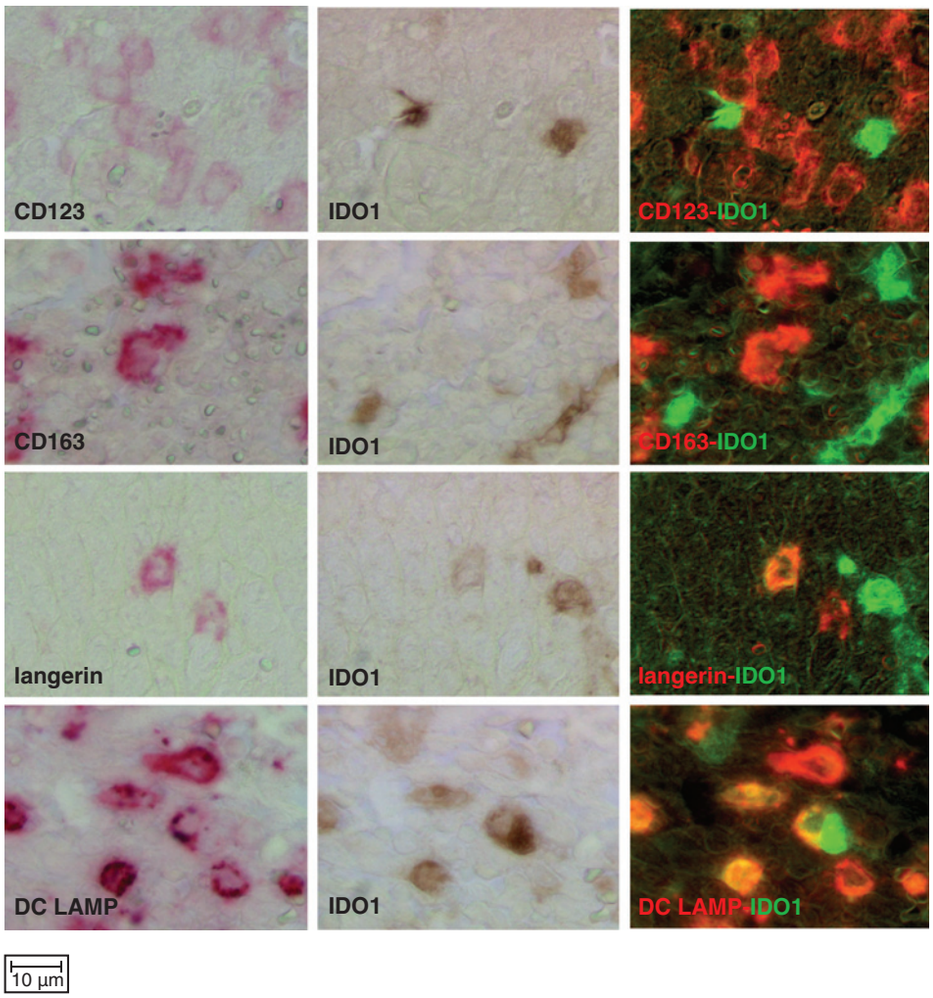

Figure 2.
Sequential IHC for characterization of IDO1$^+$ cells. First, the DC or macrophage marker (either CD123, CD163, langerin, or DC-LAMP) was labeled in red (left plots). Images were captured, coordinates were recorded, and red chromogen was removed. Next, IDO1 was detected using our rabbit polyclonal antibody revealed in brown (middle plots), and a second image was captured at each stored coordinate. The two captured images were processed into a single pseudocolor picture (red for DC/macrophage marker and green for IDO1). Colocalization of red and green signals is shown in yellow.

CsIHC, IDO1-expressing cells in the lymph nodes did not express CD123 (Fig. 2A), Langerin (Fig. 2B), and CD163 (Fig. 2C), but expressed DC-LAMP (Fig. 2D) and CD83 (not shown), thereby confirming that they are interdigitating DCs. Single- and double-positive cells were quantified in the tissue sections, and the proportion of IDO1$^+$ cells was calculated in each cell subset (Fig. 3). The results indicate that the vast majority (90%–100%) of IDO1$^+$ cells expressed DC-LAMP, whereas about 60% of DC-LAMP$^+$ cells expressed IDO1. Similarly, most IDO1$^+$ cells expressed CD83, and 30% to 40% of CD83$^+$ cells expressed IDO1. Most IDO1$^+$ cells were negative for CD1a, langerin, CD123, and CD163. These results indicate that most IDO1$^+$ cells in lymph nodes are mature DCs, whereas not all mature DCs express IDO1. Our data did not confirm the reported expression of IDO1 by human CD123$^+$ plasmacytoid DCs (18, 20–22).

Characterization of IDO1-positive cells in TDLNs

To verify previous published results showing that IDO1$^+$ cells were more abundant in TDLNs than in control lymph nodes (21), we repeated the analysis with our 4.16H1 antibody. We selected TDLNs from 15 patients with melanoma and 15 patients with breast carcinoma, whose characteristics are described in Supplementary Table S2, and are comparable with previous reported work (21). IDO1$^+$ cells were present in the TDLNs, but their numbers were not different from those observed in normal lymph nodes, as estimated by the relative area occupied by IDO1$^+$ cells (Fig. 4). The number of IDO1$^+$ cells was not affected by the presence of tumor cells in some of the lymph nodes (metastatic lymph nodes; Fig. 4). To detect possible changes in the nature of IDO1$^+$ cells in TDLNs, we performed CsIHC for IDO1, using the in-house rabbit polyclonal anti-IDO1 antibody, and antibodies against DC-LAMP, CD83, CD1a, Langerin, CD123, or CD163. As in normal lymph nodes, IDO1$^+$ cells in TDLNs corresponded mainly to DC-LAMP$^+$ CD83$^+$ DCs and not to CD123$^+$ plasmacytoid DCs (Fig. 3). We conclude that the number and nature of IDO1$^+$ cells in TDLNs do not differ from those in the normal lymph nodes. The enrichment reported previously may have resulted from a lack of specificity of the antibody used. In fact, some of these studies used antibody AB5968, which we found to have cross-reactivity with an unknown protein (Supplementary Fig. S1; refs. 18, 21, 22).

Expression of IDO1 by *in vitro*–derived DCs

Because lymph nodes contain IDO1$^+$ mature DCs, we tested whether human DCs derived *in vitro* from monocytes also express IDO1 upon maturation. Monocyte-derived DCs were matured

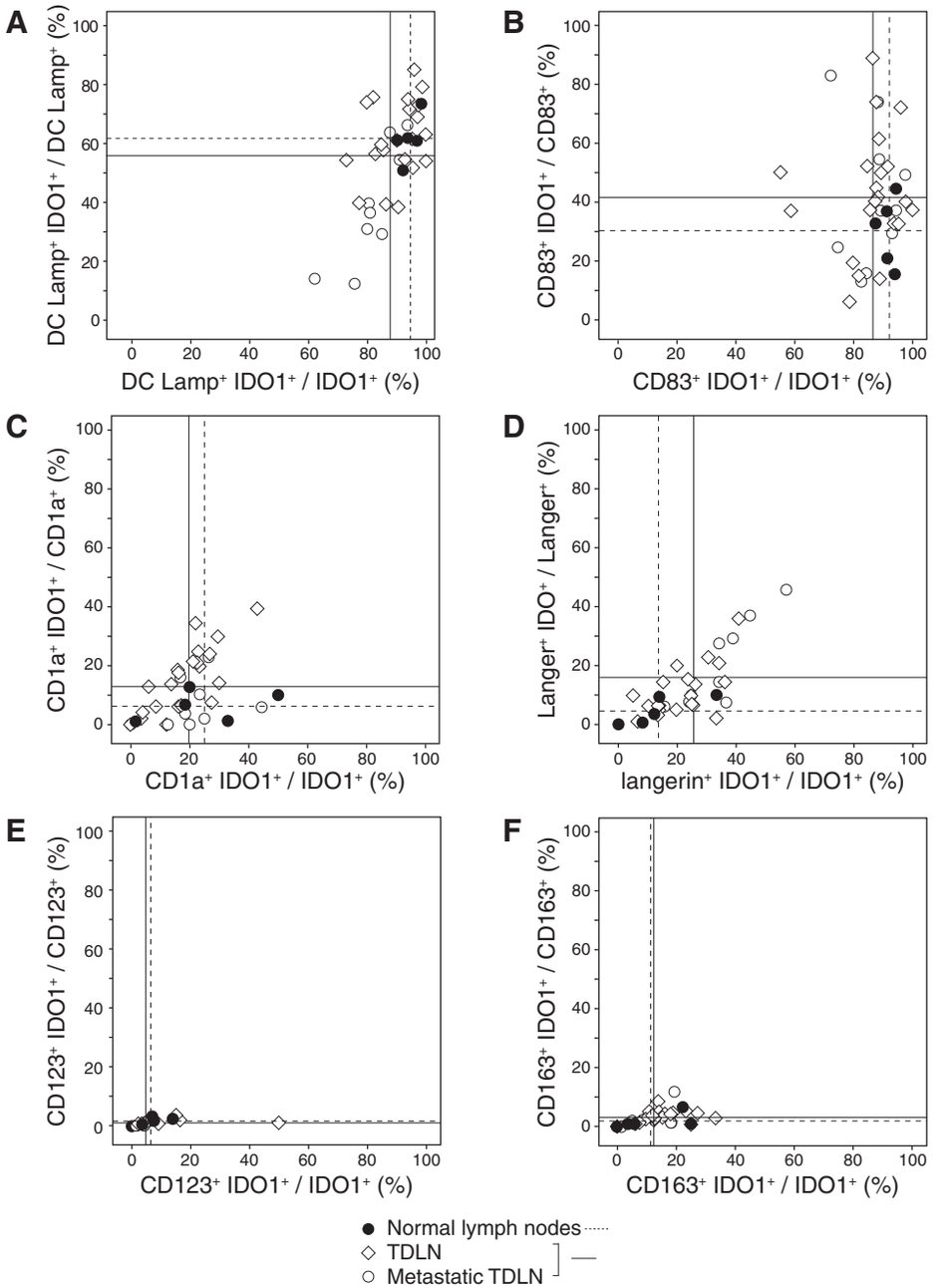

Figure 3.
Phenotypic characterization and quantification of IDO1$^+$ cells in normal lymph nodes and TDLNs. Computerized sequential IHC was used to stain normal lymph nodes and TDLNs for both IDO1 and either DC-LAMP (A), CD83 (B), CD1a (C), langerin (D), CD123 (E), or CD163 (F). Single- and double-positive–stained cells were counted. The graphs plot proportions of doubly stained cells among cells expressing either IDO1 or the other marker. Dotted and solid lines indicate mean counts in normal lymph nodes and TDLNs, respectively.

using either LPS or a cocktail of IL1β, IL6, TNFα, and PGE2, commonly used to produce DC-based vaccines for clinical immunotherapy. As reported previously by others, iDCs did not express IDO1, whereas both types of mature DCs did (Supplementary Fig. S3A). The latter were able to degrade tryptophan and produce kynurenine, indicating that IDO1 was functional in these mature DCs (Supplementary Fig. S3B). This activity was blocked by 1-methyl-L-tryptophan, a known IDO1 inhibitor, and not by its enantiomer 1-methyl-D-tryptophan, confirming the lack of inhibition of IDO1 by the latter (37, 38). When we added mature-DC conditioned medium to CD4$^+$ T cells activated with coated anti-CD3 antibody, we observed that T-cell proliferation was prevented, whereas it was maintained with the immature DC-conditioned medium (Supplementary Fig. S3B). This proliferation was maintained when the conditioned medium was obtained from mature DCs incubated with 1-methyl-L-tryptophan, but not with 1-methyl-D-tryptophan. Similar results were obtained with cocultures of T cells and DCs, in contrast with a previous report describing a positive effect of 1-methyl-D-tryptophan in this experimental setting (ref. 39; Supplementary Fig. S4). PGE2 was previously found to be able to induce IDO1 expression in human DCs (17). Accordingly, we observed that among the different factors present in the cytokine cocktail, PGE2 was critical to induce IDO1 expression, as a cocktail containing IL1β, IL6, TNFα, but no PGE2, induced DC maturation without IDO1 expression (Supplementary Fig. S3A and S3B).

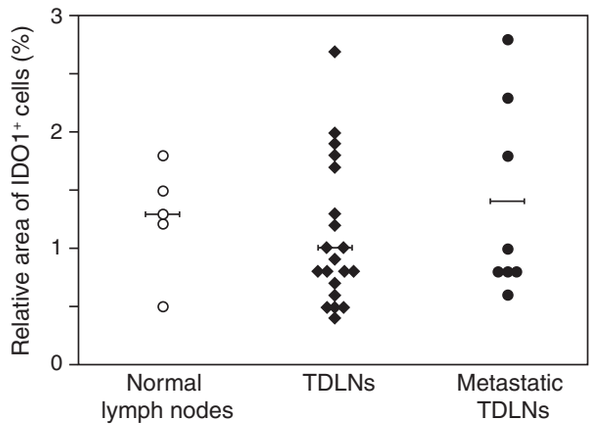

Figure 4.
Computer-assisted quantitative analysis of relative area of IDO1$^+$ cells in normal lymph nodes and TDLNs. Lymph node FFPE sections were stained with the 4.16H1 antibody. Five hot spot fields of each case were analyzed by measuring the ratio of IDO1 surface staining to overall tissue surface. Horizontal bars represent mean values.

In an effort to explain the paradoxical expression of IDO1, an immunosuppressive factor, in mature DCs, which are supposed to effectively trigger immune responses, we hypothesized that IDO1 induction might be a late step in the DC maturation program as a negative feedback aimed at preventing excessive T-cell activation. We conducted a detailed kinetic study of DC maturation by LPS, monitoring the acquisition of maturation markers, the production of stimulatory cytokines, and the induction of IDO1 at the protein level (Supplementary Table S3). The detailed kinetics, shown in Supplementary Fig. S5, was used to calculate the time required to reach 50% (T_{50}) or 100% (T_{100}) of the maximal induction after addition of the maturation signal. The earliest sign of maturation was the production of TNFα, which reached a maximum at 4 hours and has a T_{50} of less than 2 hours. The second was the production of IL10, with a T_{50} of 3.5 hours. Surface maturation markers reached a maximum at 54 hours, with T_{50} ranging between 7 and 28 hours. Maximal induction of IDO1 was observed at 46 hours, with a T_{50} of 8.7 hours. These results indicate that IDO1 induction is concomitant with the acquisition of surface maturation signals, occurring in the second part of the DC maturation program, after the induction of the earliest cytokines. Of note, no expression of *TDO2* or *IDO2*, an *IDO1* homologous gene, was observed at any time point (Supplementary Fig. S5A).

Frequency and pattern of expression of IDO1 in human tumors

We used IHC with our 4.16H1 antibody to assess IDO1 expression in 15 common solid tumor types. About 60 samples of each were investigated on TMA sections. In total, 505 of 866 tumors (58%) showed positive staining, often limited to a small number of cells (Table 2 and Fig. 5). Endometrial and cervical carcinomas most frequently expressed IDO1, followed by kidney, non–small cell lung, and colorectal carcinomas. Most glioblastomas were negative. Three different cell types were stained: tumor cells, endothelial cells in the tumor stroma, and some scattered cells in lymphocyte-rich stromal areas resembling the IDO1$^+$ mature DCs observed in lymphoid tissues. The proportion of these staining patterns varied widely according to the tumor type. For example, renal cell carcinomas showed a dominant vascular staining pattern, whereas DC-like staining predominated in colorectal tumors. IDO1$^+$ tumor cells were particularly frequent in endometrial and cervical carcinomas. Interestingly, these malignancies displayed a different distribution of IDO1$^+$ tumor cells. In cervical tumors, they were often present at the outer limit of the tumor area in contact with stroma, whereas they were more diffusely distributed in endometrial tumors (Fig. 5A and B).

We confirmed the IHC screening data with *IDO1* gene expression levels for each tumor type retrieved from the RNA-Seq data of the TCGA public database. The tumor hierarchy was remarkably consistent between the two datasets (Table 2 and Supplementary Fig. S6).

Discussion

This work provides an extensive, detailed, and comparative overview of the expression profile of IDO1 in human normal

Table 2. Frequency and pattern of expression of IDO1 in common human solid malignancies assessed by IHC on tissue microarrays

Tumor type	Number of tumor samples tested	IDO1 protein expression				
		Positive in tumor cells	Positive in blood vessels	Positive in lymphocyte-rich stroma	Positive (total)	Positive (%)
Endometrial carcinomas	48	27	15	35	45	94
Cervix carcinomas	58	32	8	40	48	83
Kidney carcinomas	60	0	40	16	48	80
Non–small cell lung carcinomas	57	13	29	38	45	79
Colorectal carcinomas	59	8	7	45	46	78
Stomach carcinomas	59	12	1	43	45	76
Ovarian carcinomas	53	9	5	18	35	66
Bladder urothelial carcinomas	58	9	3	35	36	62
Melanomas	60	18	15	28	32	53
Head and neck carcinomas	59	10	0	24	27	46
Esophageal carcinomas	60	11	0	21	25	42
Prostate carcinomas	60	11	1	19	25	42
Pancreatic carcinomas	58	9	0	15	22	38
Breast carcinomas	57	3	0	21	21	37
Glioblastomas	60	2	0	4	5	8
Total	**866**	**174**	**124**	**402**	**505**	58

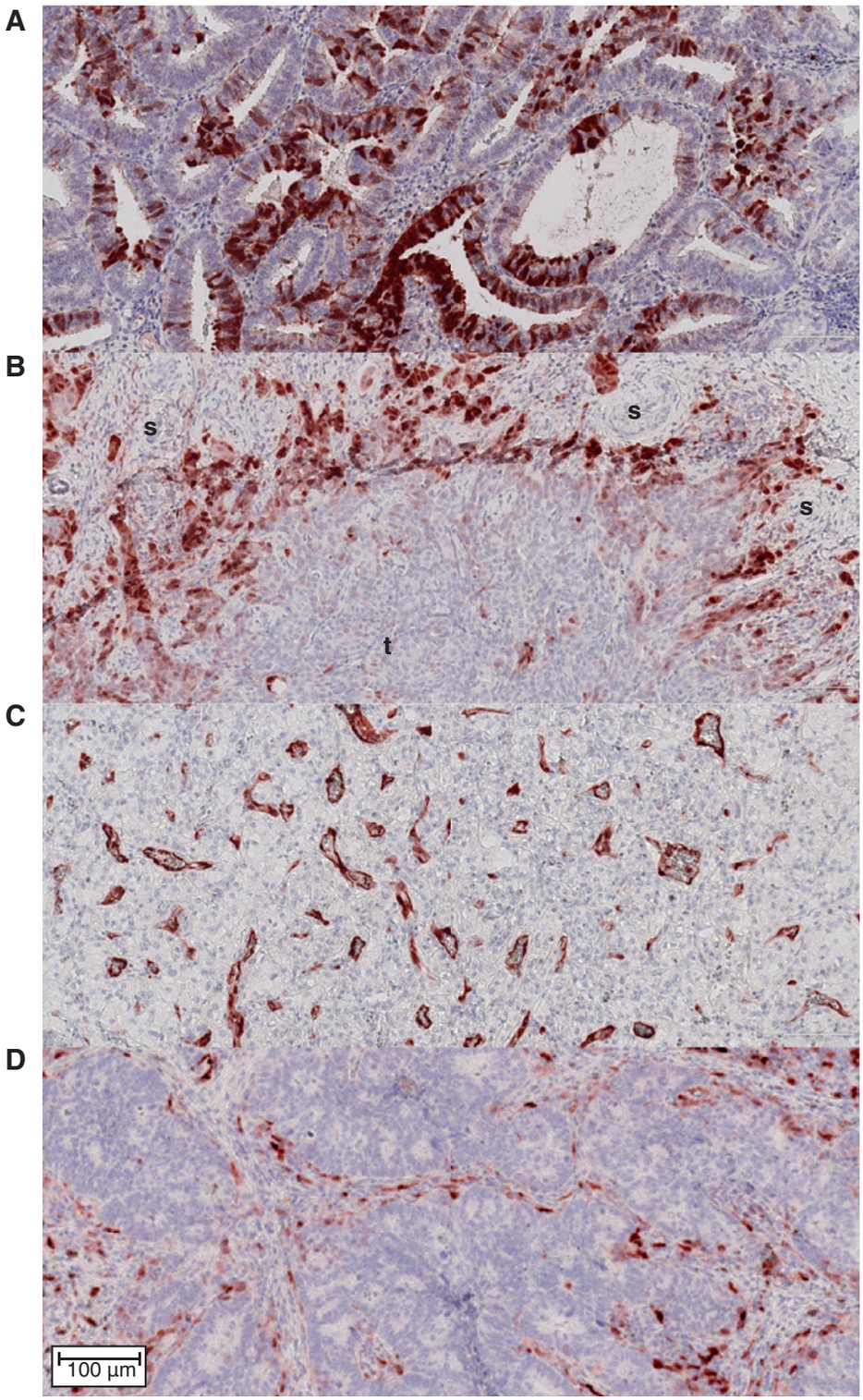

Figure 5.
IDO1 protein expression in human tumors assessed by IHC. Illustrative images from FFPE tissue sections of an endometrial adenocarcinoma (A), a cervical squamous cell carcinoma (B), in which the tumor (t) and stromal (S) parts are indicated, a renal cell carcinoma (C), and a gastric adenocarcinoma (D) stained with the anti-IDO1 antibody 4.16H1. Immunolabeled cells are stained in dark red (AEC staining). They correspond to tumor cells (A and B), endothelial cells (C), and inflammatory stromal cells (D). Each image represents 3% of the surface of large, 5-mm-wide TMA sections.

and cancerous tissues. Such an overview, unprecedented in the existing literature, is in our view helpful to harness the role of this enzyme in tumor resistance to immune rejection, and to select the most appropriate types of tumors for targeted pharmacologic inhibition of IDO1 aimed at restoring effective antitumoral immunity. To this end, and because we felt that a number of available anti-IDO1 antibodies lacked the required specificity, we have developed a new anti-IDO1 mAb, have

strictly validated its specificity, and have used it to screen a large panel of normal and tumoral tissues by IHC. Our results are consistent with a range of published observations but do not confirm other reported concepts, such as the enrichment of $IDO1^+$ DCs in human TDLNs and the expression of IDO1 by $CD123^+$ plasmacytoid DCs (18, 20–23). This latter observation has already been questioned by others (40, 41). Our new antibody might be a helpful IHC tool in translational and clinical research, to test IDO1 expression in tumor samples to correctly assess its prognostic impact, select patients for IDO1 inhibitor therapy, and study the mechanisms of tumor response to such treatments.

IDO1 expression in human tumors is restricted to three different cell types: myeloid cells, endothelial cells, and tumor cells. This specific expression has already been reported individually for each of these cell types. We show that different $IDO1^+$ cell types can coexist in individual tumors, and that the proportion of these three types can vary widely from one tissue or tumor to the other. The functional consequences of this cellular specificity, particularly in terms of inhibition of T-cell responses, are unknown.

IDO1 expression in DCs and other APCs such as macrophages has been abundantly reported and investigated. DC-mediated tryptophan catabolism is often regarded as the main mechanism by which this enzyme interferes with T-cell activity. In tissue sections, $IDO1^+$ cells often appear as individual cells scattered in lymphocyte-rich areas present in stromal or lymphoid tissues. Importantly, these structures are observed in both healthy and tumoral tissues. In the latter, they are found in all tumor types, with higher proportions in cervical, colorectal, and gastric carcinomas. It is unclear at this stage whether $IDO1^+$ myeloid cells are more abundant in tumors as compared with noncancerous inflammatory tissues, and whether they play a preferential protective role against antitumoral immune responses. It will be important to go further into this comparison, because IDO1-inhibitory drugs aimed at restoring antitumoral immunity carry a theoretical risk of inducing autoimmune side effects.

IDO1 is expressed by endothelial cells in a large proportion of placental and pulmonary blood vessels, and in a minority of blood vessels in some other organs. The function of IDO1 in endothelial cells is not known. Its metabolite kynurenine has been shown to have vasodilatory properties (42). Thus, vascular-related side effects of pharmacologic IDO1 inhibition are possible. In tumors, vascular IDO1 expression is frequent in renal cell carcinoma, whereas it is absent from breast, esophagus, head and neck, and pancreatic carcinomas. It is remarkable that normal kidneys do not host $IDO1^+$ blood vessels, as opposed to their malignant counterpart. IDO1 expression by endothelial cells was reported to be associated with a relatively more favorable prognosis in renal cell carcinomas, in contrast with other tumor types (43). Thus, treatment of kidney tumors with IDO1 inhibitors might result in paradoxical tumor-promoting effects. Additional experimental investigations are required to highlight the functional significance of endothelial IDO1 expression as well as its role in cellular immune responses.

IDO1 expression by tumor cells varies widely according to the tumor type. The proportion of tumors comprising $IDO1^+$ tumor cells ranges from zero (in renal cell carcinoma) to about 30% (in endometrial and cervical carcinomas). These proportions are lower than in our previous report that used a polyclonal antibody on a small panel of samples and may have overestimated tumoral IDO1 expression (10). In contrast, the IHC data reported here were obtained using a specific mAb on a large panel of tumors, and are further validated by the remarkable consistency with the TCGA data. This brings confidence in our current IHC data, despite the fact that we used TMA and not whole tumor sections. The molecular mechanisms underlying IDO1 expression in tumor cells are starting to be studied (44). In cervical carcinomas, IDO1 is frequently expressed by outer tumor cells in contact with the tumor stroma. It is possible that environmental factors, such as inflammatory cytokines produced in the stroma, trigger IDO1 expression in these tumor cells. Conversely, the expression is often diffuse in endometrial tumors, suggesting that the activation of the *IDO1* gene in these tumors is constitutive rather than induced by environmental factors. The fact that some human tumor cell lines constitutively express functional IDO1 is consistent with this (10). Tumor cell expression of IDO1 appears as an attractive target for IDO1 inhibitors, because it provides a direct mechanism of tumor protection against attack by contacting or closely located T cells.

Disclosure of Potential Conflicts of Interest

P. Moulin is the director of investigative pathology for Novartis Institutes of Biomedical Research. B.J. Van den Eynde has ownership interest in, and is a consultant/advisory board member for, iTeos Therapeutics.

Authors' Contributions

Conception and design: I. Théate, N. van Baren, L. Pilotte, B.J. Van den Eynde
Development of methodology: I. Théate, N. van Baren, L. Pilotte, P. Larrieu, J.-C. Renauld, C. Hervé, C. Sempoux
Acquisition of data (provided animals, acquired and managed patients, provided facilities, etc.): I. Théate, N. van Baren, L. Pilotte, P. Moulin, P. Larrieu, J.-C. Renauld, I. Gutierrez-Roelens, E. Marbaix, C. Sempoux
Analysis and interpretation of data (e.g., statistical analysis, biostatistics, computational analysis): I. Théate, N. van Baren, L. Pilotte, P. Moulin, P. Larrieu, C. Sempoux, B.J. Van den Eynde
Writing, review, and/or revision of the manuscript: I. Théate, N. van Baren, L. Pilotte, P. Moulin, J.-C. Renauld, C. Hervé, I. Gutierrez-Roelens, E. Marbaix, C. Sempoux, B.J. Van den Eynde
Administrative, technical, or material support (i.e., reporting or organizing data, constructing databases): I. Théate, I. Gutierrez-Roelens, E. Marbaix
Study supervision: N. van Baren, L. Pilotte, B.J. Van den Eynde

Acknowledgments

The authors thank Vincent Stroobant for HPLC analysis, Etienne De Plaen for RT-qPCR experiments, Marjorie Mercier, Aurélie Daumerie, and Hélène Pollet for expert assistance, and Julie Klein for editorial help.

Grant Support

This work was supported by Ludwig Cancer Research and grants from the Belgian Programme on Interuniversity Poles of Attraction initiated by the Belgian State, Prime Minister's Office, Science Policy Programming, the Belgian Cancer Plan (Action 29_049), the Fonds National pour la Recherche Scientifique (Belgium), the Fondation contre le Cancer (Belgium), the Fondation Salus Sanguinis (Belgium), and the Fonds Maisin (Belgium). The IDO1 expression screening on tumor TMAs was supported by iTeos Therapeutics.

The costs of publication of this article were defrayed in part by the payment of page charges. This article must therefore be hereby marked *advertisement* in accordance with 18 U.S.C. Section 1734 solely to indicate this fact.

Received July 18, 2014; revised September 16, 2014; accepted September 16, 2014; published OnlineFirst September 30, 2014.

References

1. Takikawa O, Yoshida R, Kido R, Hayaishi O. Tryptophan degradation in mice initiated by indoleamine 2,3-dioxygenase. J Biol Chem 1986;261: 3648–53.
2. Yamazaki F, Kuroiwa T, Takikawa O, Kido R. Human indolylamine 2,3-dioxygenase. Its tissue distribution, and characterization of the placental enzyme. Biochem J 1985;230:635–8.
3. Blaschitz A, Gauster M, Fuchs D, Lang I, Maschke P, Ulrich D, et al. Vascular endothelial expression of indoleamine 2,3-dioxygenase 1 forms a positive gradient towards the feto-maternal interface. PLoS ONE 2011;6:e21774.
4. Taylor MW, Feng GS. Relationship between interferon-gamma, indoleamine 2,3-dioxygenase, and tryptophan catabolism. FASEB J 1991;5: 2516–22.
5. Munn DH, Mellor AL. Indoleamine 2,3 dioxygenase and metabolic control of immune responses. Trends Immunol 2013;34:137–43.
6. Platten M, Wick W, Van den Eynde BJ. Tryptophan catabolism in cancer: beyond IDO and tryptophan depletion. Cancer Res 2012;72: 5435–40.
7. Baban B, Chandler P, McCool D, Marshall B, Munn DH, Mellor AL. Indoleamine 2,3-dioxygenase expression is restricted to fetal trophoblast giant cells during murine gestation and is maternal genome specific. J Reprod Immunol 2004;61:67–77.
8. de Faudeur G, de Trez C, Muraille E, Leo O. Normal development and function of dendritic cells in mice lacking IDO-1 expression. Immunol Lett 2008;118:21–9.
9. Munn DH. Prevention of allogeneic fetal rejection by tryptophan catabolism. Science 1998;281:1191–3.
10. Uyttenhove C, Pilotte L, Theate I, Stroobant V, Colau D, Parmentier N, et al. Evidence for a tumoral immune resistance mechanism based on tryptophan degradation by indoleamine 2,3-dioxygenase. Nat Med 2003;9: 1269–74.
11. Holmgaard RB, Zamarin D, Munn DH, Wolchok JD, Allison JP. Indoleamine 2,3-dioxygenase is a critical resistance mechanism in antitumor T cell immunotherapy targeting CTLA-4. J Exp Med 2013;210: 1389–402.
12. Pallotta MT, Orabona C, Volpi C, Vacca C, Belladonna ML, Bianchi R, et al. Indoleamine 2,3-dioxygenase is a signaling protein in long-term tolerance by dendritic cells. Nat Immunol 2011;12:870–8.
13. Liu X, Shin N, Koblish HK, Yang G, Wang Q, Wang K, et al. Selective inhibition of IDO1 effectively regulates mediators of antitumor immunity. Blood 2010;115:3520–30.
14. Heitger A. Regulation of expression and function of IDO in human dendritic cells. Curr Med Chem 2011;18:2222–33.
15. Wolf B, Posnick D, Fisher JL, Lewis LD, Ernstoff MS. Indoleamine-2,3-dioxygenase enzyme expression and activity in polarized dendritic cells. Cytotherapy 2009;11:1084–9.
16. Chung DJ, Rossi M, Romano E, Ghith J, Yuan J, Munn DH, et al. Indoleamine 2,3-dioxygenase-expressing mature human monocyte-derived dendritic cells expand potent autologous regulatory T cells. Blood 2009;114:555–63.
17. Braun D, Longman RS, Albert ML. A two-step induction of indoleamine 2,3 dioxygenase (IDO) activity during dendritic-cell maturation. Blood 2005;106:2375–81.
18. Munn DH. Potential regulatory function of human dendritic cells expressing indoleamine 2,3-dioxygenase. Science 2002;297: 1867–70.
19. Gerlini G, Di Gennaro P, Mariotti G, Urso C, Chiarugi A, Pimpinelli N, et al. Indoleamine 2,3-dioxygenase+ cells correspond to the BDCA2+ plasmacytoid dendritic cells in human melanoma sentinel nodes. J Investig Dermatol 2009;130:898–901.
20. Chen W, Liang X, Peterson AJ, Munn DH, Blazar BR. The indoleamine 2,3-dioxygenase pathway is essential for human plasmacytoid dendritic cell-induced adaptive T regulatory cell generation. J Immunol 2008;181: 5396–404.
21. Lee JR, Dalton RR, Messina JL, Sharma MD, Smith DM, Burgess RE, et al. Pattern of recruitment of immunoregulatory antigen-presenting cells in malignant melanoma. Lab Invest 2003;83: 1457–66.
22. Munn DH, Sharma MD, Hou D, Baban B, Lee JR, Antonia SJ, et al. Expression of indoleamine 2,3-dioxygenase by plasmacytoid dendritic cells in tumor-draining lymph nodes. J Clin Invest 2004;114: 280–90.
23. Brody JR, Costantino CL, Berger AC, Sato T, Lisanti MP, Yeo CJ, et al. Expression of indoleamine 2,3-dioxygenase in metastatic malignant melanoma recruits regulatory T cells to avoid immune detection and affects survival. Cell Cycle 2009;8:1930–4.
24. Speeckaert R, Vermaelen K, Van Geel N, Autier P, Lambert J, Haspeslagh M, et al. Indoleamine 2,3-dioxygenase, a new prognostic marker in sentinel lymph nodes of melanoma patients. Eur J Cancer 2012;48: 2004–11.
25. Mansfield AS, Heikkila PS, Vaara AT, Smitten von KA, Vakkila JM, Leidenius MH. Simultaneous Foxp3 and IDO expression is associated with sentinel lymph node metastases in breast cancer. BMC Cancer 2009;9:231.
26. Kudo Y, Boyd CA. Human placental indoleamine 2,3-dioxygenase: cellular localization and characterization of an enzyme preventing fetal rejection. Biochim Biophys Acta 2000;1500:119–24.
27. Kudo Y, Boyd CAR, Spyropoulou I, Redman CWG, Takikawa O, Katsuki T, et al. Indoleamine 2,3-dioxygenase: distribution and function in the developing human placenta. J Reprod Immunol 2004;61: 87–98.
28. Ligam P, Manuelpillai U, Wallace EM, Walker D. Localisation of indoleamine 2,3-dioxygenase and kynurenine hydroxylase in the human placenta and decidua: implications for role of the kynurenine pathway in pregnancy. Placenta 2005;26:498–504.
29. Sedlmayr P, Blaschitz A, Wintersteiger R, Semlitsch M, Hammer A, MacKenzie CR, et al. Localization of indoleamine 2,3-dioxygenase in human female reproductive organs and the placenta. Mol Hum Reprod 2002;8:385–91.
30. Santoso DIS, Rogers P, Wallace EM, Manuelpillai U, Walker D, Subakir SB. Localization of indoleamine 2,3-dioxygenase and 4-hydroxynonenal in normal and pre-eclamptic placentae. Placenta 2002;23:373–9.
31. Hönig A, Rieger L, Kapp M, Sütterlin M, Dietl J, Kämmerer U. Indoleamine 2,3-dioxygenase (IDO) expression in invasive extravillous trophoblast supports role of the enzyme for materno-fetal tolerance. J Reprod Immunol 2004;61:79–86.
32. Godin-Ethier J, Hanafi LA, Piccirillo CA, Lapointe R. Indoleamine 2,3-dioxygenase expression in human cancers: clinical and immunologic perspectives. Clin Cancer Res 2011;17:6985–91.
33. Nizet Y, Gillet L, Schroeder H, Lecuivre C, Louahed J, Renauld JC, et al. Antibody production by injection of living cells expressing non self antigens as cell surface type II transmembrane fusion protein. J Immunol Meth 2011;367:70–7.
34. Lemaire MM, Vanhaudenarde A, Nizet Y, Dumoutier L, Renauld J-C. Induction of autoantibodies against mouse soluble proteins after immunization with living cells presenting the autoantigen at the cell surface in fusion with a human type 2 transmembrane protein. J Immunol Meth 2011;367:56–62.
35. Pilotte L, Larrieu P, Stroobant V, Colau D, Dolusic E, Frederick R, et al. Reversal of tumoral immune resistance by inhibition of tryptophan 2,3-dioxygenase. Proc Natl Acad Sci U S A 2012;109: 2497–502.
36. Thomas S, DuHadaway J, Prendergast GC, Laury-Kleintop L. Specific in situ detection of murine indoleamine 2, 3-dioxygenase. J Cell Biochem 2014;115:391–6.
37. Löb S, Königsrainer A, Schafer R, Rammensee H-G, Opelz G, Terness P. Levo- but not dextro-1-methyl tryptophan abrogates the IDO activity of human dendritic cells. Blood 2008;111:2152–4.
38. Qian F, Villella J, Wallace PK, Mhawech-Fauceglia P, Tario JD, Andrews C, et al. Efficacy of levo-1-methyl tryptophan and dextro-1-methyl tryptophan in reversing indoleamine-2,3-dioxygenase-mediated arrest of T-cell proliferation in human epithelial ovarian cancer. Cancer Res 2009;69:5498–504.
39. Hou D-Y, Muller AJ, Sharma MD, DuHadaway J, Banerjee T, Johnson M, et al. Inhibition of indoleamine 2,3-dioxygenase in dendritic cells by stereoisomers of 1-methyl-tryptophan correlates with antitumor responses. Cancer Res 2007;67:792–801.
40. Terness P, Chuang J-J, Bauer T, Jiga L, Opelz G. Regulation of human auto- and alloreactive T cells by indoleamine 2,3-dioxygenase (IDO)-

producing dendritic cells: too much ado about IDO? Blood 2005;105: 2480–6.
41. Löb S, Ebner S, Wagner S, Weinreich J, Schafer R, Königsrainer A. Are indoleamine-2,3-dioxygenase producing human dendritic cells a tool for suppression of allogeneic T-cell responses? Transplantation 2007; 83:468–73.
42. Wang Y, Liu H, Mckenzie G, Witting PK, Stasch J-P, Hahn M, et al. Kynurenine is an endothelium derived relaxing factor produced during inflammation. Nat Med 2010;16:279–85.
43. Riesenberg R, Weiler C, Spring O, Eder M, Buchner A, Popp T, et al. Expression of indoleamine 2,3-dioxygenase in tumor endothelial cells correlates with long-term survival of patients with renal cell carcinoma. Clin Cancer Res 2007;13:6993–7002.
44. Litzenburger UM, Opitz CA, Sahm F, Rauschenbach KJ, Trump S, Winter M, et al. Constitutive IDO expression in human cancer is sustained by an autocrine signaling loop involving IL-6, STAT3 and the AHR. Oncotarget 2014;5:1038–51.